### Title

Ocular silicon distribution and clearance following intravitreal injection of porous silicon microparticles




### Authors

Nieto, Alejandra
Hou, Huiyuan
Sailor, Michael J
et al.



### Publication Date

2013-11-01

### DOI

10.1016/j.exer.2013.09.001

Peer reviewed

Published in final edited form as:
*Exp Eye Res*. 2013 November ; 116: . doi:10.1016/j.exer.2013.09.001.

# Ocular silicon distribution and clearance following intravitreal injection of porous silicon microparticles

**Alejandra Nieto**[a,b,1], **Huiyuan Hou**[a,b,1], **Michael J. Sailor**[b], **William R. Freeman**[a], and **Lingyun Cheng**[a,*]

Lingyun Cheng: cheng@eyecenter.ucsd.edu

[a]Jacobs Retina Center at Shiley Eye Center at University of California, San Diego, USA

[b]Department of Chemistry and Biochemistry, University of California, San Diego, USA

## Abstract

Porous silicon (pSi) microparticles have been investigated for intravitreal drug delivery and demonstrated good biocompatibility. With the appropriate surface chemistry, pSi can reside in vitreous for months or longer. However, ocular distribution and clearance pathway of its degradation product, silicic acid, are not well understood. In the current study, rabbit ocular tissue was collected at different time point following fresh pSi (day 1, 5, 9, 16, and 21) or oxidized pSi (day 3, 7, 14, 21, and 35) intravitreal injection. In addition, dual-probe simultaneous microdialysis of aqueous and vitreous humor was performed following a bolus intravitreal injection of 0.25 mL silicic acid (150 μg/mL) and six consecutive microdialysates were collected every 20 min. Silicon was quantified from the samples using inductively coupled plasma-optical emission spectroscopy. The study showed that following the intravitreal injection of oxidized pSi, free silicon was consistently higher in the aqueous than in the retina (8.1 ± 6.5 vs. 3.4 ± 3.9 μg/mL, $p = 0.0031$). The area under the concentration-time curve (AUC) of the retina was only about 24% that of the aqueous. The mean residence time was 16 days for aqueous, 13 days for vitreous, 6 days for retina, and 18 days for plasma. Similarly, following intravitreal fresh pSi, free silicon was also found higher in aqueous than in retina (7 ± 4.7 vs. 3.4 ± 4.1 μg/mL, $p = 0.014$). The AUC for the retina was about 50% of the AUC for the aqueous. The microdialysis revealed the terminal half-life of free silicon in the aqueous was 30 min and 92 min in the vitreous; the AUC for aqueous accounted for 38% of the AUC for vitreous. Our studies indicate that aqueous humor is a significant pathway for silicon egress from the eye following intravitreal injection of pSi crystals.

### Keywords

intravitreal porous silicon; ocular silicon clearance; ocular drug delivery; rabbit eye

## 1. Introduction

Retinal diseases are often chronic and refractory to treatment. Two unique challenges in developing drugs against these diseases derive from the inherent barriers that prevent drugs in the blood from reaching the retina and from the short vitreous half-life of drugs



*Corresponding author. Department of Ophthalmology, Jacobs Retina Center at Shiley Eye Center, University of California, San Diego, 9415 Campus Point Drive, La Jolla, CA 92093-0946, USA. Tel.: +1 858 534 3780; fax: +1 858 534 7985.
[1]Both authors contributed equally to this work.

**Financial disclosure**: A. Nieto, None; H. Hou, None; M.J. Sailor, Spinnaker Biosciences (I); W.R. Freeman, Spinnaker Biosciences (C); L. Cheng, Spinnaker Biosciences (C).

administered via intravitreal injection. This makes necessary frequent drug administration if directly injected into the eye, entailing the risk of infection and other complications. A major focus in our research is to devise strategies for bypassing this barrier and developing ocular drug delivery systems able to provide sustained drug levels to the retina (Cheng et al., 2004; Chhablani et al., 2013).

Mesoporous silicon microparticles have been proposed as a drug delivery vehicle to achieve a slow drug release and a long-lasting therapeutic effect. (Anglin et al., 2008; Salonen et al., 2008), (Kashanian et al., 2010) In general, porous silicon has demonstrated good biocompatibility. (Bimbo et al., 2010) However, biocompatibility is dependent on location and tissue types (Leoni et al., 2002; Park et al., 2009) as well as surface chemistry of the porous silicon particles. (Low et al., 2006) The eye is a unique organ with clear media that offers a direct view of compounds or delivery systems injected into the vitreous. The eye is especially suitable for a porous silicon drug delivery system because the direct imaging of porous silicon particles may enable non-invasive monitoring of payload release from the nanoscale pores. (Wu et al., 2011) We previously showed that intravitreally injected porous silicon particles were not toxic in rabbit eyes, showing good biocompatibility and slow elimination from the body. (Cheng et al., 2008) Elimination of micron-size particles of porous silicon from the eye necessarily involves degradation of the material into water-soluble products. The degradation of porous silicon *in vivo* involves two main processes: oxidation of the elemental silicon component and dissolution of the silicon oxide thus formed. The soluble silicon-containing species are various protonated forms of the orthosilicate ion, $SiO_4^{4-}$, and its oligomers. The form of orthosilicate that predominates at neutral pH is silicic acid $Si(OH)_4$, which is naturally found in numerous tissues. Silicon is considered an essential trace element and in aqueous environment at neutral pH, $Si(OH)_4$ is excreted from the body through the urine (Mertz, 1981). For the purpose of ocular drug delivery, a significant quantity of porous silicon particles needs to be placed in the vitreous. It is therefore important to assess the fate of the silicic acid degradation product of the particles. The ocular distribution and clearance pathway of silicic acid has not yet been documented. This issue is not only of academic interest, but it is also a practical issue to better understand this ocular drug delivery system and possible safety issues associated with higher doses and longer-term exposure of ocular tissues involved in the clearance pathway of silicic acid. Theoretically, porous silicon particles degrade in the vitreous and the final product, silicic acid, may be removed from the eye through the retina to the choroid then to systemic circulation or through the aqueous humor to Schlemm's canal and then to systemic circulation. The surface chemistry plays an important role in the rate at which particles degrade; as-prepared porous silicon degrades faster than material whose surface has been modified by oxidization or hydrosilylation (Cheng et al., 2008). The purpose of the present study was to determine the ocular elimination kinetics and pathways of silicon clearance from the eye for two important formulations of porous silicon microparticles: as-prepared particles (pSi) which consist of Si–Si and Si–H bonds, and thermally oxidized porous silicon particles ($pSiO_2$) which contain Si–O–Si bonds as the primary structural motif. The correlation of pSi degradation with drug release will depend on individual drug loaded such as daunorubicin shown previously by us (Wu et al., 2011). However, the silicon clearance pathway is independent to payload and is the objective of the current study.

## 2. Materials and methods

### Porous silicon (pSi) microparticle preparation

Porous Si (pSi) microparticles were prepared by anodic electrochemical etch of highly doped, (100)-oriented, p-type silicon wafers (boron-doped, 1.10 mΩ·cm resistivity; obtained from Siltronix Inc., Archamps, France), in an electrolyte consisting of a 3:1 (v:v) solution of

48% aqueous hydrofluoric acid (HF) and ethanol (Fisher-Scientific, Pittsburg, PA). A Si wafer with an exposed area of 8.04 $cm^2$ was contacted on the back side with a strip of aluminum foil and mounted in a Teflon etching cell that was fitted with a platinum counter electrode. The wafer was etched using a current density waveform ($J$) previously described: (Wu et al., 2011) $J = A_0 + A \cdot \cos(kt + a)$, where $A_0$ is current density offset (mA/$cm^2$), $A$ is current density amplitude (mA/$cm^2$), $k$ is frequency ($s^{-1}$), $t$ is time (s), and $a$ is phase shift ($s^{-1}$). The values used for $A_0$, $A$, and $a$ were 90.2 mA/$cm^2$,12.4 mA/$cm^2$, and 0, respectively. The current density waveform generates a porosity modulation in the porous silicon layer that acts as a 1-dimensional photonic crystal. (Vincent, 1994), (Thonissen and Berger, 1997) The photonic crystal displays a sharp peak in the optical reflectance spectrum whose wavelength is directly proportional to $k$. The value of $k$ was adjusted to yield a reflectance peak whose maximum occurred in the spectrum at ∼600 nm; a typical value for $k$ was 2.25. The waveform was etched into the silicon wafer for a total of 400 s. The resulting porous layer was then removed from the silicon substrate by replacing the electrolyte with a 1:29 (v:v) solution of 48% aqueous hydrofluoric acid and ethanol and then applying an anodic pulse (6.2 mA/$cm^2$) for 120 s. Each wafer was subjected to four such etching protocols, and the porous layers were collected and ultrasonicated in ethanol for 30 min in an FS5 dual action ultrasonic cleaner (Thermo Fisher Scientific, Pittsburg, PA), then rinsed with ethanol 3 times.

### Porous silicon oxide ($pSiO_2$) microparticle preparation

The $pSiO_2$ formulation was prepared from pSi by air oxidation in a ceramic boat inside a muffle furnace (Thermo Fisher Scientific, Pittsburg, PA). The temperature in the furnace was increased from room temperature to 800 °C at a heating rate of 10 °C $min^{-1}$ and then held in air for 1 h. The furnace was allowed to cool to room temperature for an additional 3 h prior to removal of the samples. The oxidation reaction was accompanied by a color change of the particles from brown to transparent, corresponding to conversion of Si to $SiO_2$ in the porous matrix. However, the particle size and shape were not affected by the oxidation procedure. For sustained ocular drug delivery purposes, we have found that oxidized porous silicon shows a longer vitreous half-life (Cheng et al., 2008) and the surface is more amenable to covalent functionalization for subsequent drug grafting (Chhablani et al., 2013).

### Physical characterization of porous microparticles

Average particle size and pore size were determined from plan-view images of randomly selected particles ($n > 10$) using a Phillips XL30 field emission scanning electron microscope operating at an accelerating voltage of 5 kV (FEI Phillips, Hillsboro, OR). Surface chemistry was characterized by Fourier transform infrared (FTIR) spectroscopy using attenuated total reflectance (ATR) mode on a Nicolet 6700 Smart-iTR spectrometer (Thermo Fisher Scientific, Pittsburg, PA). The textural properties of the particles were analyzed by nitrogen adsorption at −196 °C on an ASAP 2020 porosimetry apparatus (Micromeritics, Norcross, GA). Prior to the adsorption experiment, approximately 50 mg of the porous Si sample was outgassed overnight at 105 °C. The specific surface area and pore volume of the particles were calculated from the $N_2$ adsorption isotherms using the BET (Brunauer-Emmett-Teller) and BJH (Barrett-Joyner-Halenda) methods, respectively (Gregg and Sing, 1982), (Brunauer et al., 1938; M. Kruk and Jaroniec, 1999).

### Animal studies

All animal experiments were carried out in adherence to ARVO Statement for the Use of Animals in Ophthalmic and Vision Research.

1) Ocular pharmacokinetic tissue sampling: Forty pigmented rabbits were used for the study and only one eye of each rabbit was used for microparticle intravitreal injection. Out of 40

rabbits, 20 were used for the fresh porous silicon (pSi) particle study and the other 20 were used for the oxidized porous silicon ($pSiO_2$) particle study. For the pSi particle study, 1 mg of pSi particles in 100 μL of balanced salt solution (BSS; Thermo Fisher Scientific, Pittsburg, PA) was injected into the right eye of each of the 20 rabbits using a 27 gage needle. At the post-injection time points day 1, 5, 9, 16, and 21, four rabbits were subjected to a comprehensive eye exam, including anterior segment biomicroscopy, posterior indirect ophthalmoscopy and intraocular pressure (IOP) measurements, before the planned sacrifice. Four animals at each time point were used to account for the inherent variation of pSi microparticle suspension concentration injected as well as variation between individual animals. Immediately after sacrifice, the enucleated eye globes were dissected individually into aqueous, vitreous, and retina as described previously (Cheng et al., 2004; Nan et al., 2010). For the $pSiO_2$ particle study, 2 mg of particles in 100 μL of BSS were injected with a 27 gage needle and a longer study course was performed because of the slower dissolution property of $pSiO_2$ microparticles (Cheng et al., 2008). The rabbits injected with the $pSiO_2$ particles were sacrificed at post-injection day 3, 7, 14, 21, and 35, four animals at each time point. Prior to both intravitreal injection and the scheduled sacrifice, 1 mL of blood was sampled for silicon quantitation. The collected eye tissues and plasma were kept at −80 °C until the quantitation of Si (as dissolved silicic acid) was performed by inductively coupled plasma-optical emission spectroscopy (ICP-OES).

2) Simultaneous microdialysis of aqueous and vitreous humor: To better understand the distribution and elimination of orthosilicate from the eye, a dual-probe microdialysis was performed as previously described (Chen et al., 2013). For this acute study, one rabbit was used (3.7 kg body weight). The rabbit had a comprehensive eye exam before the microdialysis experiment. After general anesthesia with intramuscular ketamine (35 mg/kg body weight) and xylazine (6.25 mg/kg body weight) and topical anesthesia with proparacaine hydrochloride (Ophthalmic solution USP 0.5% (wt/vol); Bausch & Lomb, Rochester, NY), an anterior chamber microdialysis probe (CMA 30 linear, 4 mm membrane length custom made, 6000 Da molecular weight cut-off; CMA Microdialysis, North Chelmsford, MA) was installed followed by installation of a vitreous microdialysis probe (CMA 20 Elite, 4 mm membrane length, 20,000 Da molecular weight cut-off; CMA Microdialysis, North Chelmsford, MA). Tissue adhesive (Vetbond 1469SB; 3M Corporation, St Paul, MN) was applied around the probe entry point to prevent ocular fluid leaks. Thirty minutes after the installation of the probes, intravitreal injection of 0.250 mL of silicic acid solution (150 μg/mL) was performed to yield final vitreous concentration of 25 μg/mL, assuming rabbit vitreous volume to be 1.5 mL The saturated stock silicic acid solution was prepared by dissolving 5 mg pure silicic acid crystals (Spectrum Laboratory Products, Gardena, CA) in 10 mL 50 mM sodium hydroxide (NaOH; Sigma–Aldrich, St Louis, MO) in phosphate buffered saline solution (PBS; Thermo Fisher Scientific, Pittsburg, PA) and incubated at 37 °C for one week. The solution pH was adjusted to 7 with hydrochloric acid (HCl; Sigma–Aldrich, St Louis, MO) before intravitreal injection of the supernatant. During the microdialysis experiment, both probes were perfused with PBS at 1 μL/min using a microsyringe pump (NE-100; New Era Pump Systems Inc, Farmingdale, NY). The vitreous and aqueous perfusate samples were collected every 20 min for total of 6 collections. During the course of the microdialysis experiment, the rabbit remained on a water blanket (TP650; Gaymar Industries, Orchard Park, NY) to help prevent body heat loss and anesthesia was maintained by boosting every 40 min using one half volume of the first dose. Every other dose was ketamine only starting with the first boost because xylazine stays in the system longer (Veilleux-Lemieux et al., 2012). At the end of the microdialysis procedure, a blood sample was acquired before the animal was sacrificed and the eye globe enucleated. The eye globe was dissected under a surgical microscope to sample aqueous humor, vitreous humor, and retina. These eye tissues were separately stored at −80 °C until silicon was quantitated using ICP-OES.

After the *in vivo* microdialysis experiment, the probes were placed in deionized water (WFI-quality, cell culture grade, Cellgro, Manassas, VA) for continued flushing overnight to clean the silicic acid from the system before performing a test to determine the recovery rate of silicon for the probes. For this purpose, each probe was soaked in a vial of 25 (μg/mL silicic acid solution and the perfusate was collected every 20 min for 6 consecutive times.

## Silicon quantification

To determine the silicon content as dissolved silicon (silicic acid) in the aqueous and vitreous, the collected fluid samples were weighed and centrifuged at 11,000 rpm for 10 min. Aqueous fluid supernatant (0.1 mL) was diluted with 2% (v/v) nitric acid aqueous solution to make a final volume of 3 mL ($HNO_3$; EMD, Darmstad, Germany). Vitreous fluid supernatant (0.07 mL) was diluted with 2% (v/v) $HNO_3$ aqueous solution to make a final volume of 3 mL (Park et al., 2009), (Dyck et al., 2000; Hauptkorn et al., 2001; Wills et al., 2008) To determine the silicon content in the retina tissue, the wet samples were weighed and digested with hydrogen peroxide 30% (w/w) (0.05 mL) ($H_2O_2$; Sigma–Aldrich, St. Louis, MO) and concentrated $HNO_3 \sim 15.7$ M (0.250 mL) for 2 days. To determine the silicon concentration in plasma, 0.150 mL of sample was digested with a solution consisting of 0.025 mL of 30% (by mass) aqueous $H_2O_2$ and 0.125 mL of concentrated $HNO_3$ for 2 days. Mechanical homogenization of the tissue samples was performed with a pellet pestle (Sigma–Aldrich, St. Louis, MO) applied for 10 s after addition of the digesting reagents, resulting in a homogeneous slurry. The digested tissues were centrifuged at 11,000 rpm for 10 min and the supernatant (0.1 mL) was diluted with 2% (v/v) $HNO_3$ aqueous solution to make a final volume of 3 mL This open vessel digestion procedure with $HNO_3$–$H_2O_2$ was designed to ensure that as much of the analyte that is available for recovery is rendered soluble and relatively stable in aqueous acidic medium. Silicon calibration standard solutions were prepared from a stock solution containing 1000 μg/mL Si (Trace Cert Silicon standard for ICP in nitric acid; Fluka, Milwaukee, WI). External calibration standard solutions were prepared in 2% (v/v) $HNO_3$ solution in water (WFI-quality, cell culture grade; Cellgro, Manassas, VA) by serial dilution to reach final concentrations 8, 4, 2,1, 0.5, 0.1 and 0.01 μg/mL Calibration standards and samples were prepared in polystyrene tubes. Normal rabbit aqueous, vitreous, retina and plasma from rabbits that had not received any injection of pSi or $pSiO_2$ particles (InVision BioResources, Seattle, WA) were treated following the same procedure as the samples and used as controls to determine the baseline levels of silicon.

Soluble silicon, in the form of protonated orthosilicate species, was detected by inductively coupled plasma-optical emission spectroscopy (ICP-OES) in an argon plasma spectrometer (Optima 3000 DV; Perkin–Elmer, Norwalk, CT) equipped with a standard torch, Scott-type spray chamber, GemTip cross-flow nebulizer and an AS-90 autosampler (Perkin–Elmer, Norwalk, CT). The ICP-OES instrument parameters are summarized in Table 1.

## Data analysis

Pharmacokinetic (PK) parameters of silicon content in ocular tissues and plasma were calculated using non-compartmental methods and sparse sampling setting within the Phoenix® WinNonlin® software (version 6.3; Pharsight Corp, Mountain View, CA). The area under the curve from time zero to the last measurable concentration ($AUC_{0-t}$) was calculated. A terminal rate constant of elimination was calculated using a minimum of three measurable concentrations and a terminal elimination half-life was calculated using 0.693/*k*el. The pharmacokinetic parameters of silicon content from the microdialysis of vitreous and aqueous humor were calculated using the PK software module using a one-compartment model and IV-Bolus input setting. For comparison of silicon concentrations detected among the ocular tissues, the data from all the time points of the same tissue were pooled and

nonparametric multiple comparison (each pair using Wilcoxon method) was performed using JMP statistical software (version 10; SAS Institute Inc, Cary, NC).

## 3. Results

### Porous silicon particle characterization

The pSi and $pSiO_2$ particles displayed an average particle size of 43 × 70 × 25 μm and an average pore size of ∼13 nm in the electron microscope images (Fig. 1). Particle size and shape were not affected by the oxidation procedure.

The FTIR spectrum of pSi microparticles display bands characteristic of surface hydride species. A band at 2110 $cm^{-1}$ associated with the ν Si-H stretching vibrations, a band corresponding to the $\delta$ Si-$H_2$ scissors mode at 910 $cm^{-1}$, and a band corresponding to a ν Si-H deformation mode (665 $cm^{-1}$) are apparent in the spectrum (Fig. 2, line tracing at the bottom). For the $pSiO_2$ formulation, complete oxidation of the porous Si matrix to porous $SiO_2$ was verified *ex situ* by the appearance of a broad band centered at 1000 $cm^{-1}$ in the FTIR spectrum, associated with silicon-oxide stretching modes (Fig. 2, line tracing at the top).

The $N_2$ adsorption/desorption isotherms of the pSi and $pSiO_2$ microparticles are plotted in Fig. 3. The isotherms exhibit type IV hysteresis loops with parallel adsorption and desorption branches suggesting cylindrical mesopores of approximately constant cross section. The measured surface area decreases after oxidation, from 454 ± 5 $m^2$/g for pSi to 207 ± 4 $m^2$/g for $pSiO_2$ microparticles. The total pore volume decreases from 1.3 $cm^3$/g for pSi to 0.6 $cm^3$/g for $pSiO_2$.

### Clinical Exams

The eyes injected with the oxidized particles did not show any abnormalities at any time points following the injection. Two eyes out of the twenty eyes injected with fresh pSi particles were found with mild vitreous cloudiness and aqueous trace cells (4–5 cells per millimeter square) on their scheduled sacrifice days (day 9 and day 16). The rabbit eyes at the other time points were normal. The intraocular pressure (IOP) was comparable between the injected eyes and their fellow eyes (for pSi particles, OD IOP = 9.4 ± 2.0 *vs* OS IOP = 10.2 ± 2.6 mmHg, $p = 0.46$, *t* Test; for $pSiO_2$ particles, OD IOP = 7.5 ± 1.7 *vs* OS IOP = 8.2 ± 1.3 mmHg, $p = 0.27$, *t* Test).

### Ocular Pharmacokinetics

**Normal silicon concentration value in eye and plasma—**The silicon concentration found in the normal rabbit aqueous humor, vitreous humor, retina, and plasma is summarized in Table 2.

**Porous silicon particles (pSi)—**The elimination of orthosilicate from the eye following a single intravitreal injection of 1 mg pSi particles is demonstrated in Fig. 4.

The ocular pharmacokinetics of Si reflects both the degradation of pSi crystals to generate aqueous silicic acid and the clearance of this soluble aqueous silicic acid product. As shown in Fig. 4, detected free silicon (in the form of aqueous silicic acid) was consistently higher in the aqueous humor (mean 7 ±4.7 μg/mL) than in the retina (mean 3.4 ± 4.1 μg/mL) ($p = 0.014$, each pair usingWilcoxon method), which suggests the aqueous humor is a significant pathway for silicon egress from the eye following an intravitreal injection. Accordingly, the area under the concentration-time curve of the retina was only about 50% of that of the aqueous humor (Table 3).

Free silicic acid concentration in the aqueous humor, the vitreous humor, and the retina was highest at the first time point (day 1) after the injection and gradually decreased over time. The mean residence time was 7 days for vitreous humor, 9 days for aqueous humor, 7 days for retina, and 11 days for plasma.

**Oxidized porous silicon particles ($pSiO_2$)—**The concentration-time traces for elimination of silicic acid from the eye following a single intravitreal injection of 2 mg of $pSiO_2$ particles is shown in Fig. 5.

Similar to the elimination data observed following intravitreal injection of pSi, the ocular elimination pharmacokinetics of $pSiO_2$ represents both the dissolution kinetics of the porous silicon matrix and the clearance of the soluble silicon product, silicic acid. As expected, the concentration of free silicic acid was the largest in the vitreous humor, and the concentration of free silicic acid was significantly larger in the aqueous humor than in the retina (vitreous mean 15 ± 9 *vs* aqueous mean 8.1 ± 6.5, $p = 0.0063$; aqueous mean *vs* retina mean of 3.4 ± 3.9, $p = 0.0031$; each pair using Wilcoxon method). The area under the concentration-time curve for the retina was only about 24% of the area under the corresponding curve for the aqueous humor (Table 4). This distribution of soluble silicon among the three ocular tissues was similar to the clearance profile observed for the pSi particle formulation.

**Microdialysis of aqueous and vitreous humor—**In experiments involving dual-probe microdialysis of vitreous and aqueous humor, the silicon was administered in its free soluble form (silicic acid) as a bolus injection into the vitreous. The recovery rate for the probe in the vitreous humor was 13% and in the aqueous humor it was only 2%. The kinetics of elimination of silicic acid from vitreous and from aqueous humor both followed a first-order one-compartment PK model (Fig. 6).

The terminal half-life of soluble silicon in the aqueous humor was 30 min and in the vitreous humor it was 92 min; the area under the concentration-time curve for aqueous humor was 1490 which was 38% of the corresponding area under the curve for vitreous humor (3950) (Table 5).

## 4. Discussion

The current study showed that elevated silicon levels were detectable in the aqueous, the vitreous, and the retina of the rabbit eyes as well as in the animal's systemic circulation following a single intravitreal injection of the pSi or $pSiO_2$ particles. It appears that the silicic acid dissolution product of the pSi or $pSiO_2$ particles in the vitreous humor migrated forward into the aqueous humor more effectively than backwards into the retina because the dissolved silicon levels were significantly larger in the aqueous humor than in the retina for both types of injected particles. The pharmacokinetic analysis demonstrated that the partitioning of silicic acid to the retina was only 24% (pSi particle study) to 50% ($pSiO_2$ particle study) of the quantity that migrated to the aqueous humor. This is in contradiction with the normal vitreous fluid elimination pathway. It is believed that vitreous water exits mainly through the retina into the choroid (over 80%) and only a very small percentage (<5%) is removed through the aqueous pathway (Moseley et al., 1984). The current results indicate that dissolved Si in the form of silicic acid may not passively diffuse along with vitreous water elimination. A similar situation has also been reported for some other small molecules by Araie and Maurice, who demonstrated that intravitreally injected fluorescein mainly leaves the vitreous compartment through the retinal surface while similarly injected fluorescein glucuronide and dextran-conjugated fluorescein isothiocyanate leaves the vitreous compartment through the vitreous–aqueous interface and the aqueous pathway (Araie and Maurice, 1991). The mechanism that favors elimination of silicic acid through

the anterior segment rather than the posterior segment is not understood at this time, although it may be related to the charge on the silicic acid species. While silicic acid ($Si(OH)_4$) is a neutral species at pH 7, it is deprotonated to form the ion $SiO(OH)_3^-$ at pH > 10. Silicic acid can also form complexes with metal cations, (Collery et al., 1998; Iler, 1979) and at high concentrations it can form larger molecular weight oligomers (Brinker and Scherer, 1990). We hypothesize that ions or complexes of mono-meric silicic acid ($Si(OH)_4$) may form in the vitreous that are less capable of penetrating the retina. It should be noted that how the degraded product (silicic acid) of porous silicon is eliminated will not affect depository property of porous silicon as a drug delivery vehicle in vitreous. How effective the payload can target retina depends on the property of the payload once leached out from porous silicon into vitreous; and how long the crystal porous silicon can last in vitreous depends on its stability imparted by surface chemistry modifications.

As mentioned above, the pharmacokinetics of pSi microparticles represents a combination of the kinetics of oxidation of silicon and dissolution of the oxide formed. The oxide on the pSi formulation is formed at physiological conditions, whereas and the oxide contained in the $pSiO_2$ formulation is prepared at 800 °C. The chemical behavior of these two oxides is expected to be quite different. Indeed, in our previous study we found that as-formed porous silicon (pSi) degrades faster than oxidized porous silicon ($pSiO_2$) when placed in rabbit vitreous (Cheng et al., 2008). The more rapid degradation of the pSi formulation is expected to yield a larger concentration of dissolved silicon in the vitreous fluid. To allow better comparison of the pSi and the $pSiO_2$ results, we therefore injected a smaller quantity of pSi particles compared to the $pSiO_2$ particles (1 mg versus 2 mg, respectively). In either case, the injected particles act as a depot that gradually degrades in the vitreous to yield a sustained concentration of dissolved silicon in all the ocular tissues studied. The non-compartmental pharmacokinetic analysis showed that both mean residence time (MRT) and terminal half-life of the $pSiO_2$ particles were larger than those of the pSi particles, which is expected due to the slower rate of $pSiO_2$ degradation *in vivo*. (Cheng et al., 2008) Though the elimination kinetics of Si in these two studies is different, in both cases the exposure of the aqueous humor to Si was significantly greater than the exposure of the retina to Si.

To confirm the findings described above we injected dissolved silicic acid into the vitreous and performed simultaneous microdialysis from the vitreous and aqueous humor. The elimination kinetics of Si from both the vitreous and the aqueous fit well to a one-compartment PK model. Si elimination from the aqueous compartment was faster (25 ng/min) and the half-life was shorter (30 min) compared with the vitreous compartment (9 ng/min and half-life of 92 min, respectively). The results are consistent with fluid turnover rates for aqueous and vitreous of rabbit in that the turnover rate in the aqueous humor is ∼4 μL/min while it is only ∼2 μL/min in the vitreous (McMaster and Macri, 1967), (Becker, 1961) (Davson and Luck, 1956). As was observed with the particle injections, we found that significant quantities of silicon transfer to the aqueous compartment: integration of the curves of Fig. 6 showed that the concentration of Si in the aqueous compartment was 38% of the concentration in the vitreous compartment. It should be noted that the microdialysis was to confirm if a significant part of intravitreally injected soluble silicic acid is indeed eliminated from the anterior chamber pathway; the vitreous or aqueous half-life of the soluble silicic acid should not be confused with the half-life of the crystal porous silicon particle.

In the current study, silicon levels measured in plasma were persistent, with a longer half-life and a longer mean residence time than in the ocular tissues. In the studies using both pSi and $pSiO_2$, silicon levels in the plasma were approx. 5 μg/mL, which is approx. 2.5 times the normal silicon level in rabbit plasma (Roberts and Williams, 1990). This persistent high level of silicon in the systemic circulation may have influenced the silicon level in the

aqueous at the later stage because the both studies showed a higher silicic acid level in aqueous humor than in vitreous humor at the later time points. This also explains that half-life or mean residence time of the soluble silicic acid was longer in aqueous than in vitreous in the eyes with depository porous silicon crystal injection.

In summary, the current study demonstrates that a significant amount of silicon is cleared through the anterior pathway or aqueous humor pathway following intravitreal injection of porous Si or porous Si oxide microparticles. Though silicon is a vital trace element in the body, the silicon concentration in systemic circulation of the normal population is low (~ 5 μmol/L, equivalent to 140 ng/mL using molecular weight of 28.086 g/mol for elemental silicon) (Jurkic et al., 2013; Roberts and Williams, 1990). Thus prolonged exposure of the eye's anterior segment such as the cornea endothelium and the endothelium of trabecular meshwork to dissolved silicon needs to be studied further beyond 12 months which was the longest observation we had so far and no toxicity was noted (Cheng et al., 2008). A limitation of the present study is that the injected amount of pSi or $pSiO_2$ particles was difficult to control precisely due to the nature of the particle suspensions, which could have led to large differences in measured concentrations between the study eyes. This is especially true for the fresh porous silicon particles, which were quite hydrophobic and dispersed poorly in the fluid phase. In an intravitreal drug delivery application, fresh porous silicon particle will not be used due to its shorter presence in vitreous humor (Cheng et al., 2008). Nonetheless, all three studies (as-formed pSi, $pSiO_2$, and dual-probe microdialysis of free silicic acid injections) showed similar results for the distribution and clearance of silicon. In particular, a significant pathway for clearance of dissolved Si (in the form of silicic acid) from the vitreous compartment is through the aqueous compartment.

## Acknowledgments

A.N acknowledges the Fundacion Alfonso Martin Escudero for a postdoctoral fellowship.

**Financial support**: This study was supported by the National Institutes of Health under grant number NIH EY020617.

## References

Anglin EJ, Cheng L, Freeman WR, Sailor MJ. Porous silicon in drug delivery devices and materials. Adv Drug Deliv Rev. 2008; 60:1266–1277. [PubMed: 18508154]

Araie M, Maurice DM. The loss of fluorescein, fluorescein glucuronide and fluorescein isothiocyanate dextran from the vitreous by the anterior and retinal pathways. Exp Eye Res. 1991; 52:27–39. [PubMed: 1714398]

Becker B. The turnover of bromide in the rabbit eye. Arch Ophthalmol. 1961; 65:837–839. [PubMed: 13688432]

Bimbo LM, Sarparanta M, Santos HA, Airaksinen AJ, Mäkilä E, Laaksonen T, Peltonen L, Lehto VP, Hirvonen J, Salonen J. Biocompatibility of thermally hydrocarbonized porous silicon nanoparticles and their biodistribution in rats. ACS Nano. 2010; 4:3023–3032. [PubMed: 20509673]

Brinker, CJ.; Scherer, GW. Sol-gel Science: the Physics and Chemistry of Sol-gel Processing. Academic Press; San Diego: 1990.

Brunauer S, Emmett PH, Teller E. Adsorption of gases in multimolecular layers. J Am Chem Soc. 1938; 60:309–319.

Chen H, Sun S, Li J, Du W, Zhao C, Hou J, Xu Y, Cheng L. Different intravitreal properties of three triamcinolone formulations and their possible impact on retina practice. Invest Ophthalmol Vis Sci. 2013; 54:2178–2185. [PubMed: 23449717]

Cheng LY, Hostetler KY, Lee J, Koh HJ, Beadle JR, Bessho K, Toyoguchi M, Aldern K, Bovet JM, Freeman WR. Characterization of a novel intraocular drug-delivery system using crystalline lipid

antiviral prodrugs of ganciclovir and cyclic cidofovir. Invest Ophthalmol Vis Sci. 2004; 45:4138–4144. [PubMed: 15505067]

Cheng L, Anglin E, Cunin F, Kim D, Sailor MJ, Falkenstein I, Tammewar A, Freeman WR. Intravitreal properties of porous silicon photonic crystals: a potential self-reporting intraocular drug-delivery vehicle. Br J Ophthalmol. 2008; 92:705–711. [PubMed: 18441177]

Chhablani J, Nieto A, Hou H, Wu EC, Freeman WR, Sailor MJ, Cheng L. Oxidized porous silicon particles covalently grafted with daunorubicin as a sustained intraocular drug delivery system. Invest Ophthalmol Vis Sci. 2013; 54:1268–1279. http://dx.doi.org/10.1167/iovs.12-11172. [PubMed: 23322571]

Collery, P.; Maymard, I.; Theophanides, T.; Khassanova, L.; Collery, T. Metal Ions in Biology and Medicine. John Libbey; Eurotext, Paris: 1998.

Davson H, Luck CP. A comparative study of the total carbon dioxide in the ocular fluids, cerebrospinal fluid, and plasma of some mammalian species. J Physiol. 1956; 132:454–464. [PubMed: 13320410]

Dyck KV, Robberecht H, Cauwenbergh RV, Deelstra H, Arnaud J, Willemyns L, Benijts F, Centeno JA, Taylor H, Soares ME, Bastos ML, Ferreira MA, D'Haese PC, Lamberts LV, Hoenig M, Knapp G, Lugowski SJ, Moens L, Riondato J, Grieken RV, Claes M, Verheyen R, Clement L, Uytterhoeven M. Spectrometric determination of silicon in food and biological samples: an interlaboratory trial. J Anal At Spectrom. 2000; 15:735–741.

Gregg, SJ.; Sing, KSW. Adsorption, Surface Area, and Porosity. second. Academic Press Inc.; London: 1982.

Hauptkorn S, Pavel J, Seltner H. Determination of silicon in biological samples by ICP-OES after non-oxidative decomposition under alkaline conditions. Fresen J Anal Chem. 2001; 370:246–250.

Iler, RK. The Chemistry of Silica. John Wiley & Sons; New York: 1979.

Jurkic LM, Cepanec I, Pavelic SK, Pavelic K. Biological and therapeutic effects of ortho-silicic acid and some ortho-silicic acid-releasing compounds: new perspectives for therapy. Nutr Metab. 2013; 10

Kashanian S, Harding F, Irani Y, Klebe S, Marshall K, Loni A, Canham L, Fan DM, Williams KA, Voelcker NH, Coffer JL. Evaluation of mesoporous silicon/polycaprolactone composites as ophthalmic implants. Acta Biomater. 2010; 6:3566–3572. [PubMed: 20350620]

Kruk M, Jaroniec M. Relations between pore structure parameters and their implications for characterization of MCM-41 using Gas Adsorption and X-ray diffraction. Chem Mater. 1999; 11:492–500.

Leoni L, Boiarski A, Desai TA. Characterization of nanoporous membranes for immunoisolation: diffusion properties and tissue effects. Biomed Microdevices. 2002; 4:131–139.

Low SP, Williams KA, Canham LT, Voelcker NH. Evaluation of mammalian cell adhesion on surface-modified porous silicon. Biomaterials. 2006; 27:4538–4546. [PubMed: 16707158]

McMaster PR, Macri FJ. The rate of aqueous humor formation in buphthalmic rabbit eyes. Invest Ophthalmol. 1967; 6:84–87. [PubMed: 6016389]

Mertz W. The essential trace-Elements. Science. 1981; 213:1332–1338. [PubMed: 7022654]

Moseley H, Foulds WS, Allan D, Kyle PM. Routes of clearance of radioactive water from the rabbit vitreous. Brit J Ophthalmol. 1984; 68:145–151. [PubMed: 6696868]

Nan KH, Sun SM, Li YL, Qu J, Li GX, Luo L, Chen H, Cheng LY. Characterisation of systemic and ocular drug level of triamcinolone acetonide following a single sub-tenon injection. Brit J Ophthalmol. 2010; 94:654–658. [PubMed: 20447969]

Park JH, Gu L, von Maltzahn G, Ruoslahti E, Bhatia SN, Sailor MJ. Biodegradable luminescent porous silicon nanoparticles for in vivo applications. Nat Mater. 2009; 8:331–336. [PubMed: 19234444]

Roberts NB, Williams P. Silicon measurement in serum and urine by direct current plasma emission spectrometry. Clin Chem. 1990; 36:1460–1465. [PubMed: 2387042]

Salonen J, Kaukonen AM, Hirvonen J, Lehto VP. Mesoporous silicon in drug delivery applications. J Pharm Sci-US. 2008; 97:632–653.

Thonissen M, Berger MG. Multilayer structures of porous silicon. Properties of Porous Silicon. 1997

Veilleux-Lemieux D, Beaudry F, Hélie P, Vachon P. Effects of endotoxemia on the pharmacodynamics and pharmacokinetics of ketamine and xylazine anesthesia in Sprague–Dawley rats. Vet Med Res Rep. 2012; 3:99–109.

Vincent G. Optical-properties of porous silicon superlattices. Appl Phys Lett. 1994; 64:2367–2369.

Wills NK, Ramanujam VMS, Kalariya N, Lewis JR, van Kuijk FJGM. Copper and zinc distribution in the human retina: relationship to cadmium accumulation, age, and gender. Exp Eye Res. 2008; 87:80–88. [PubMed: 18579132]

Wu EC, Andrew JS, Cheng L, Freeman WR, Pearson L, Sailor MJ. Real-time monitoring of sustained drug release using the optical properties of porous silicon photonic crystal particles. Biomaterials. 2011; 32:1957–1966. [PubMed: 21122914]

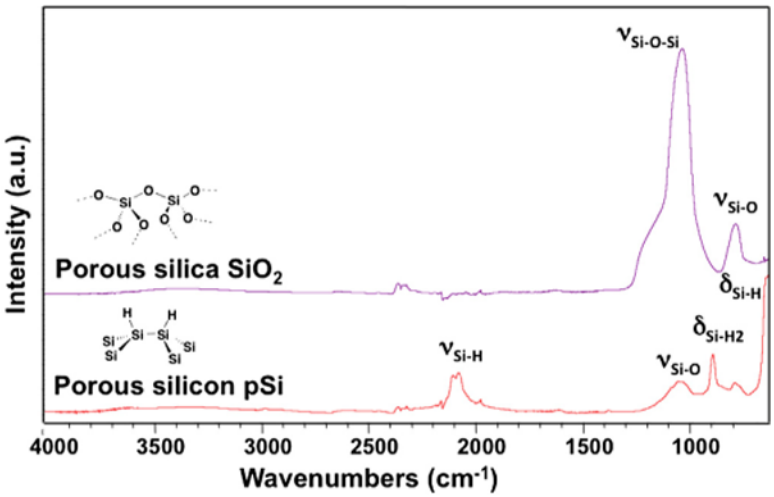


**Fig. 1.**

(a) Scanning electron microscope (SEM) image of a sample of as-prepared porous Si microparticles (pSi) (b) A close-up SEM view of one of the microparticles, showing the mesoporous structure.

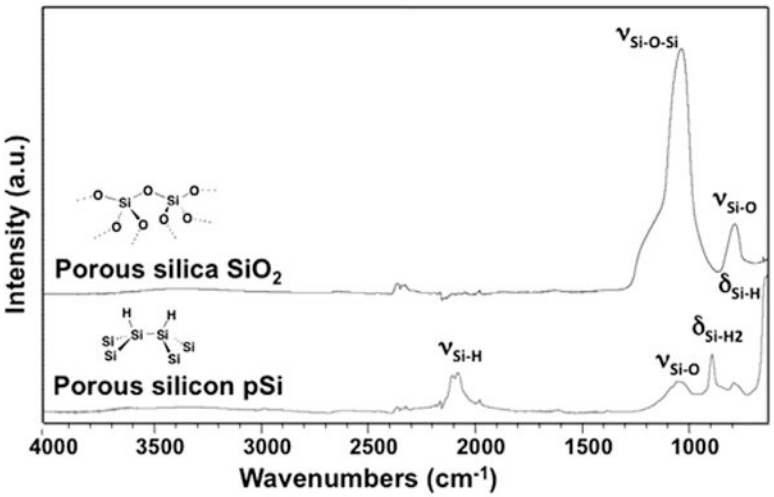


**Fig. 2.**

(a) FTIR spectra of as-prepared porous silicon (pSi) particles and oxidized porous silicon ($pSiO_2$) particles. The hydrogen-terminated surface of the as-prepared pSi particles is converted to silicon dioxide during the thermal oxidation process used to prepare $pSiO_2$.

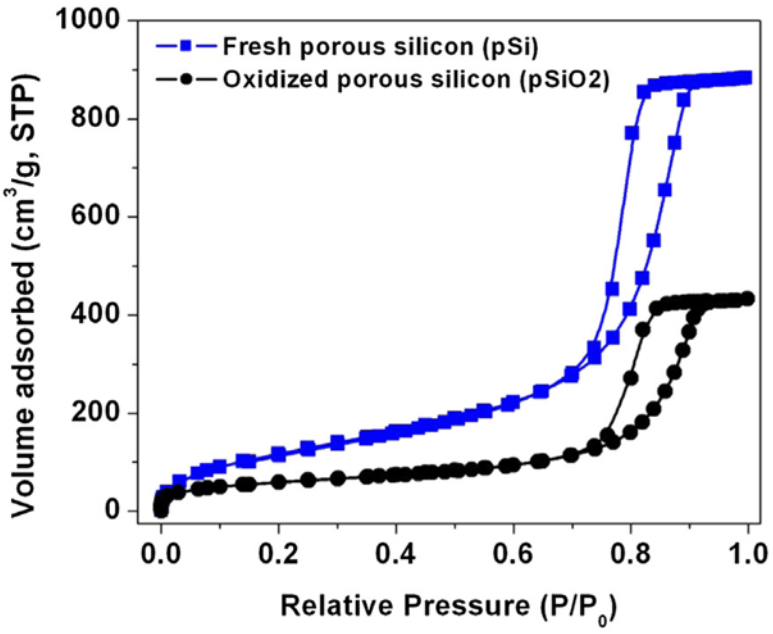


**Fig. 3.**

Nitrogen adsorption/desorption isotherms of porous silicon (pSi) and oxidized porous silicon ($pSiO_2$) microparticles.

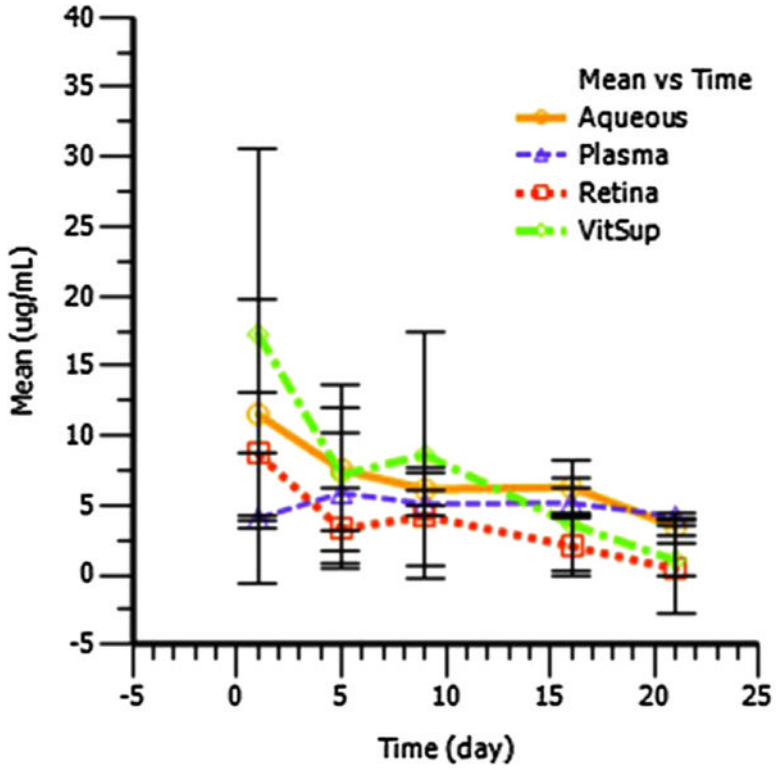


**Fig. 4.**

Concentration-time curves from the ocular tissues and the plasma after intravitreal injection of 1 mg of pSi particles. Silicon concentration in the aqueous humor (yellow solid line) was consistently higher than in the retina (red dotted line). (For interpretation of the references to colour in this figure legend, the reader is referred to the web version of this article.)

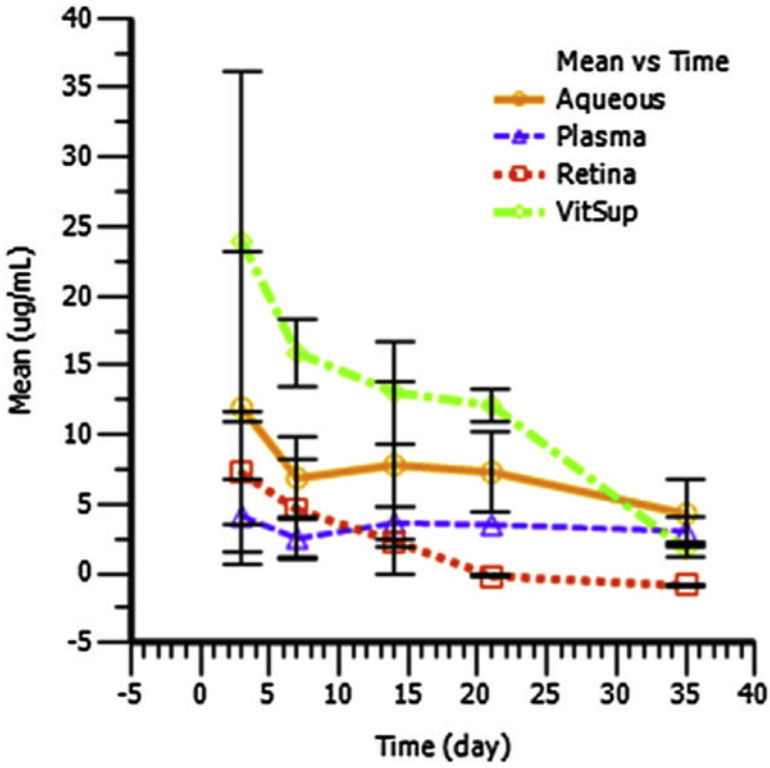


**Fig. 5.**

Concentration-time curves from the ocular tissues and the plasma after intravitreal injection of 2 mg $pSiO_2$ particles. Silicon concentration in the aqueous humor (yellow solid line) was consistently higher than in the retina (red dotted line); and silicon concentration was the highest in vitreous fluid (green interrupted line). (For interpretation of the references to colour in this figure legend, the reader is referred to the web version of this article.)

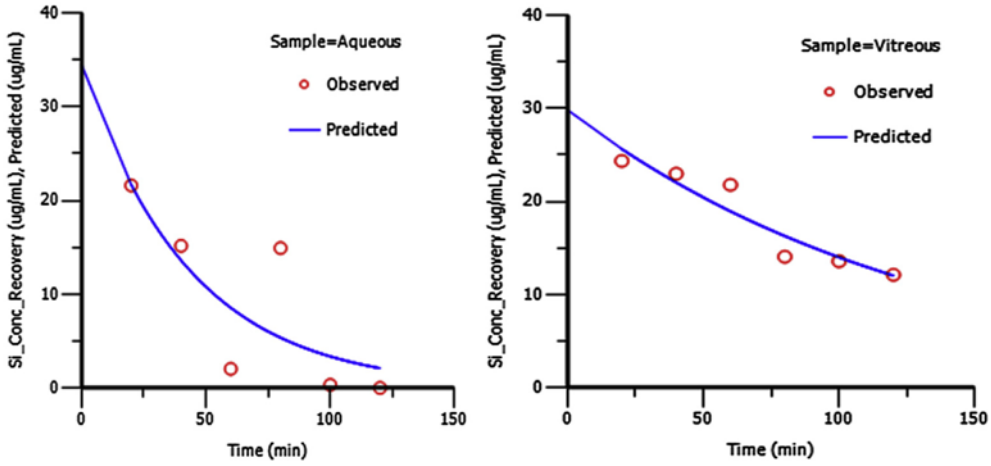


**Fig. 6.**

Concentration-time curves from the microdialysate of aqueous humor (left panel) and from vitreous humor (right panel) following a bolus intravitreal injection of 37.5 μg of soluble silicic acid into the vitreous compartment. The clearance of silicic acid from the aqueous humor was faster than from the vitreous humor.

**Table 1**

ICP-OES measurement parameters.

| | |
|---|---|
| Plasma gas (Ar) flow rate | 15 L $min^{-1}$ |
| Intermediate plasma gas (Ar) flow rate | 0.5 L $min^{-1}$ |
| Nebulizer gas (Ar) flow rate | 0.60 L $min^{-1}$ |
| Sample flow rate | 1.0 mL $min^{-1}$ |
| RF power | 1400 W |
| Pump rate | 100 rpm |
| Wash time | 30 s |
| Sample read delay time | 50 s |
| Nebulizer | Glass, concentric |
| Spray chamber | Glass, cyclonic |
| Injector | Aluminum oxide |
| Torch view | Axial |
| Background | 2-point |
| Wavelength | 251.611 nm |
| Replicates | 3 |

## Table 2

Normal silicon levels in eye tissues and plasma.

| Tissue | Concentration (μg/mL) | *n* |
|---|---|---|
| Aqueous | 1.8 ± 0.2 | 3 |
| Vitreous | 1.4 ± 0.1 | 5 |
| Retina | 2.1 ± 0.1 | 3 |
| Plasma | 1.7 ± 0.1 | 5 |

**Table 3**

Pharmacokinetic parameters following intravitreal fresh porous silicon particles.

| Tissue | $R^2$, adjusted | Half-life (day) | $T_{max}$ (day) | $C_{max}$ (μg/mL) | $AUC_{last}$ (μg day/mL) | $MRT_{last}$ (day) |
|---|---|---|---|---|---|---|
| VitSup | 0.92 | 4 | 1 | 17 | 144 | 7 |
| Aqueous | 0.62 | 17 | 1 | 12 | 140 | 9 |
| Retina | 0.81 | 4 | 1 | 9 | 72 | 7 |
| Plasma | 0.25 | 45 | 5 | 6 | 103 | 11 |

VitSup = vitreous supernatant.

$T_{max}$ = time at which the concentration was maximum.

$C_{max}$ = maximum concentration detected.

$AUC_{last}$ = area under the concentration-time curve from time 0 to the last time point.

$MRT_{last}$ = mean residence time calculated from time 0 to the last observing time point.

**Table 4**

Pharmacokinetic parameters following intravitreal oxidized porous silicon particles.

| Tissue | $R^2$, adjusted | Half-life (day) | $T_{max}$ (day) | $C_{max}$ (μg/mL) | $AUC_{last}$ (μg day/mL) | $MRT_{last}$ (day) |
|---|---|---|---|---|---|---|
| VitSup | 0.82 | 7 | 3 | 24 | 402 | 13 |
| Aqueous | 0.90 | 23 | 3 | 12 | 241 | 16 |
| Retina | 0.99 | 7 | 3 | 7 | 59 | 6 |
| Plasma | 0.96 | 80 | 3 | 4 | 112 | 18 |

VitSup = vitreous supernatant.

$T_{max}$ = time at which the concentration was maximum.

$C_{max}$ = maximum concentration detected.

$AUC_{last}$ = area under the concentration-time curve from time 0 to the last time point.

$MRT_{last}$ = mean residence time calculated from time 0 to the last observing time point.

**Table 5**

Pharmacokinetic parameters after intravitreal administration of silicic acid.

| Sample | AUC (μg min/mL) | Half-life (min) | CL (μg/min) | MRT (min) | $V_{ss}$ (mL) |
|---|---|---|---|---|---|
| Aqueous | 1490 ± 370 | 30 ± 15 | 0.025 ± 0.006 | 43 ± 21 | 0.3 ± 0.1 |
| Vitreous | 3950 ± 460 | 92 ± 17 | 0.009 ± 0.001 | 132 ± 24 | 1.3 ± 0.1 |

AUC = Area under concentration-time curve.

MRT = Mean residence time.

CL = Clearance.

$V_{SS}$ = Apparent volume of distribution at steady state.